

AERODYNAMIC, UNSTEADY, KINETIC AND HEAT LOSS EFFECTS ON THE DYNAMICS AND STRUCTURE OF WEAKLY-BURNING FLAMES

Fokion N. Egolfopoulos
Department of Mechanical Engineering
University of Southern California
Los Angeles, California 90089-1453

Introduction

Under realistic combustion conditions, flames can be unsteady and strained, exchange heat and mass through interactions with flames, combustion products and walls, and lose heat through radiation. Previous studies [1,2] have shown that the sensitivity of the flame response to strain, heat (radiative) loss, and chemical kinetics is particularly heightened for weakly-burning flames which are characterized by reduced flame temperatures and burning rates. For these flames, low activation energy termination reactions start competing strongly for the important H radicals with the high activation energy main branching reaction $H+O_2 \rightarrow OH+O$ and a critical balance between them is required for the establishment of vigorous burning. This balance can be easily lost by perturbations of the imposed strain and/or heat loss, and for premixed flames this sensitivity appears to increase as certain concentration limits are approached beyond which burning is not possible; these limits are typically referred as the lean and rich "flammability limits" [3]. The dynamic response of weakly-burning flames is of interest to turbulent combustion in which the highly non-uniform flowfields will preferentially affect and extinct the weaker flamelets first.

Premixed flames burning close to their flammable limits are characterized by slow flame speeds (of the order of 1-5 cm/s) and their experimental investigation under the influence of the earth gravity is complicated by the buoyancy-induced convection and instabilities. This has been the motivation for near-limit studies in microgravity, which have included the use of the standard flammability tube and spherical bomb. In both cases, however, the systematic accounting for the effects of the wall heat and radical losses (tube) or transient strain (spherical bomb) can not be easily obtained and the only accountable parameters are the inherently present radiative heat losses and the Lewis (Le) number effect [4,5].

The experimental configuration which provides near-adiabatic flames and the effect of strain can be systematically determined is the opposed jet counterflow [6,7]. This technique has been extensively used for experimental as well as theoretical studies on strained premixed and diffusion flames and its use has resulted to significant insight into the effects of strain on flame ignition, propagation, structure, and extinction [6-8]; experiments have only been conducted at earth gravity. Extinction studies for near limit concentrations have also resulted to an alternative method of determining flammability limits by extrapolating to zero strain the extinction strain rates at various near-limit concentrations [9]. The technique, however, has limitations when the concentrations are such that the flame speed drops below 5 cm/s and the forced convective transport is reduced. First, the whole flame ensemble is pushed upward because of the buoyant forces so that the flowfield symmetry is not preserved and the imposed strain and molecular transport are being altered. Second and more important, the upper jet becomes unstable since the less-dense fluid around the flame zone is beneath the more-dense fluid of the unreacted mixture and that causes a wavy motion which makes the whole counterflow system unstable; these effects become more severe at elevated pressures. Previous work on the pressure limits [9] by using the counterflow technique was limited to a maximum pressure of 3 atm and minimum flame speeds of the order of 5 cm/s.

The coupling of strain, radiation, and chain mechanisms can be also assessed by studying diffusion flames in a counterflow configuration in which the impinging streams are characterized by low convective velocities and, therefore, large flame thicknesses. Similarly to the premixed near-limit flames, buoyancy induces instabilities because of the existence of the more-dense jet above the less-dense flame regime.

The majority of the present knowledge on the effects of strain and heat loss and their coupling with the chemical kinetics has been obtained by studying steady flames. Unsteadiness, however is inherently present in any realistic situation and it is important that its effect is independently quantified and understood. The strain and heat loss introduce characteristic time scales which have to be simultaneously considered and compared to the characteristic transport and chemical times. Flow field unsteadiness introduces an additional time scale which further complicates the analysis. The unsteadiness can lead to permanent extinction or temporal extinction followed by reignition, depending on the magnitude of the imposed strain, flame thickness, and the frequency of oscillations [10]. Such behavior can be especially profound for weakly-burning, easy-to-extinct flames which typically have increased thicknesses.

Objectives

In view on the above considerations, the first objective of the program (initiated in June of 1994) is to introduce the meritorious counterflow methodology in microgravity in order to quantify the steady and unsteady characteristics of weakly-burning premixed and diffusion flames for a wide variety of conditions including elevated pressures. Subsequently, through detailed modeling and comparisons with the experimental data, to provide physical insight into the elementary mechanisms controlling the flame response. The configuration offers good control over the parameters of interest and can be modelled closely.

The knowledge which will be gained from the counterflow flames will be subsequently used to analyze near-limit phenomena related to other configurations by conducting detailed numerical simulations including multidimensional ones. Among the problems to be analyzed are the downward and upward propagation of near-limit flames in tubes and phenomena observed in spherical and cylindrical geometries.

Experimental Methodology

The counterflow configuration includes the use of two opposed, aerodynamically shaped nozzles from which the reactant streams emerge and impinge onto each other. The nozzles are of variable diameter ranging from 20 to 40 mm and the burner assembly is housed into a variable pressure chamber which operates between 0.1 and 10 atm. Based on the dimensions and time scales of the experiments, the 2.2 sec drop tower and the KC-135 plane will be used.

One of the innovations of the proposed experiment is the study of unsteady strained flames by oscillating the nozzle exit velocities. The flow oscillator operates through the rotation of a cylinder cut at an angle. As the cylinder turns, it smoothly opens and closes the flow passageway. The partial closure of the passage decreases the flow rate to the burners until the passage begins to open again.

The measurements include the determination of the flame location and flow velocities. The flame location is monitored by recording the flame luminous zone and a visible ruler by using high-speed cine-photography in real time. The velocity measurements constitute the most challenging part of the program, since they require laser diagnostics systems with dimensions and power requirements appropriate for the microgravity facilities. Experiments are being currently performed in the 2.2 sec drop tower, and the flame response is quantified by using the mass continuity equation and estimating global strain rates by dividing the nozzle exit velocities by the nozzle separation distance. The results of detailed numerical simulations are also being used to provide an accurate correlation between the global and local preflame strain rates. Subsequently, the Laser Doppler Velocimetry (LDV) and Digital Particle Image Velocimetry (DPIV) techniques will be implemented for the more accurate description of the velocity field.

Numerical Methodology

Numerical simulation of the counterflow is being conducted by solving the unsteady conservation equations of mass, momentum, energy, and species for the stagnation streamline in a finite domain with the addition of radiative transfer from CH_4 , H_2O , CO_2 , and CO [2,10]. The numerical simulation of spherical and cylindrical geometries is being conducted by solving the one-dimensional, unsteady, conservation equations of mass, momentum, energy, and species in the appropriate coordinates. The numerical simulation of the laminar flow in tubes is being conducted by solving the

axisymmetric unsteady conservation equations of mass, momentum, energy, and species. All codes are integrated to CHEMKIN [11] and transport [12] codes and detailed kinetics are being used.

Propagation and Extinction of Near-Limit Premixed Flames

Understanding of the behavior of near-limit premixed flames is of particular interest to lean-burn combustors and safety. The behavior of lean flames appears to have significant differences compared to near-stoichiometric flames for a number of reasons. As the fuel concentration decreases and the flammability limit is approached, substantial chemical kinetics and Le number effects become important. The lower flame temperature starts favoring low activation energy reactions which typically have retarding effects on burning [1]. At the same time, the fuel becomes the deficient species and the magnitude of its mass diffusivity becomes a critical factor on the flame response to fluid mechanics [4,5]. Furthermore, the effect of thermal radiation starts becoming important since the magnitude of the radiative losses becomes comparable to the heat release rate. Thus, the burning rate is reduced [1] and extinction is facilitated [2] significantly compared to their adiabatic counterparts as it also shown in Figs. 1 and 2 respectively. Lean flames are also particularly sensitive to pressure variations due to the kinetic imbalance between two-body and three-body reactions which significantly affect the overall burning intensity.

Dynamics of Weakly-Burning Diffusion Flames

The application of aerodynamic straining on a diffusion flame, results to reactant leakage and flame temperature reduction which eventually can lead to flame extinction. Furthermore, as the straining increases, the mass burning rate increases and the thickness of the flame transport zone decreases. Contrary to premixed flames, whose burning rate is controlled by the flame speed, the burning rate of diffusion flames can be arbitrarily augmented by increasing the convective fluxes. By reducing the value of the convective transport of the reactant streams towards zero, the thickness of the diffusion flame increases and the radiation heat transfer is enhanced.

The effect of radiation on the extinction of strained counterflow diffusion flames due to the reduction of the methane mass fraction, Y_{CH_4} , in the fuel stream can be seen in Fig. 3 for various nozzle exit velocities, u_{exit} [2]. In Fig. 3a, $u_{exit}=180$ cm/s which results to large K (200 to 250 s⁻¹) and, therefore, small flame thickness. It can be seen that as Y_{CH_4} is reduced, the maximum flame temperature, T_{max} , is reduced and extinction is obtained at sufficiently low Y_{CH_4} values as indicated by the rapid reduction of the T_{max} . However, the overall response of the flame to Y_{CH_4} variations minimally depends on radiation. This indicates that for flames with small thickness, the magnitude of the radiative loss is reduced and its effect on the flame characteristics and extinction is not crucial.

In Fig. 3b, the results correspond to $u_{exit}=5$ cm/s which results to substantially reduced K (about 1 s⁻¹), and, therefore, increased flame thickness. The results demonstrate that the inclusion of the radiative loss mechanism indeed affects the flame response as indicated by the substantial reduction of the T_{max} , and the different Y_{CH_4} values at extinction. Such effect is due to the increased magnitude of the radiative loss as induced by the increased flame thickness and, therefore, increased volume of the radiating species. In Fig. 3b, results are also shown for 5 atm flames and it is seen that as the pressure increases, the T_{max} increases and that the temperature reduction due to radiation increases. This is reasonable since the gas emissivity increases directly proportional with pressure. Furthermore, it is seen that the limit Y_{CH_4} values at extinction are higher for the 5 atm case. This happens because as extinction is approached, the three-body main termination reaction ($H+O_2+M \rightarrow HO_2+M$) is favored over the two-body main branching reaction ($H+O_2 \rightarrow OH+O$) and extinction is facilitated at larger Y_{CH_4} values.

The results presented herein demonstrate that there can be a significant coupling between the processes of straining and radiation as the strain rate is reduced significantly. Such conditions can be encountered in situations of flame spread since no substantial strain is applied on the flame surface while it spreads.

3. Unsteady and Radiation Effects on Weakly-Burning Strained Flames

The effect of radiative loss under the presence of unsteady strain rate has also been examined for both premixed and diffusion flames [2]. For the premixed flames, cases close to the lean flammability

limit were studied. For the diffusion flames, conditions allowing for elevated and near zero strain rates during a cycle were examined.

In Fig. 4, the effects of unsteady strain and radiation on the dynamic response of a $\phi=0.5$ CH₄/air atmospheric flame are shown in terms of the variation of the value of the maximum heat release, Q_{max} , versus a non-dimensional time, t' , resulting from the scaling of the real time with the period. It can be seen that by conducting adiabatic calculations, the flame responds in a sinusoidal manner to the imposed sinusoidal u_{exit} variations and permanent extinction does not occur. More specifically, Q_{max} , which is directly proportional to the mass flux under vigorous burning conditions, assumes its peak (trough) value when u_{exit} is at its peak (trough) value. The inclusion of radiation, however, leads to reduced flame strength and permanent extinction is obtained at low frequencies. At higher frequencies, extinction is either delayed or suppressed and that depends on the relative magnitudes of the time required for extinction and the time during which the flame remains into the "unfavorable" strain regime [10]. For the 1 Hz adiabatic and the 40 Hz radiative cases, it can be seen that although permanent extinction does not occur, partial extinction and subsequent reignition occur as indicated by the reduction and subsequent increase of Q_{max} at the high strain part of the cycle.

In Fig. 5, the effect of unsteady strain and radiation on the response of a diffusion flame is shown. The results have been obtained for a mean $u_{exit,O}=30$ cm/s and an amplitude $u_{exit,A}=25$ cm/s which results to peak and trough values of u_{exit} equal to 55 and 5 cm/s respectively, and, therefore, to large variations of the flame thickness throughout the cycle. For this reason, it was conjectured that when $u_{exit}=5$ cm/s the radiation will be enhanced compared to the $u_{exit}=55$ cm/s condition. This is indeed shown in Fig. 5a in which the variation of the maximum flame temperature, T_{max} , is shown as function of t' . It can be seen that, at low frequencies, as the u_{exit} is reduced from its mean value, T_{max} initially increases because of the reduced O₂ leakage through the main reaction zone. This increase, however, is subsequently arrested and a reduction of T_{max} is observed although u_{exit} keeps decreasing, and this is due to the radiation effect which results from the increased flame thickness as u_{exit} is reduced. Subsequently, T_{max} reaches a local minimum and then starts increasing again at the regime at which u_{exit} starts increasing, leading, therefore, to reduced flame thickness and radiative loss. This T_{max} increase is subsequently arrested at the point at which u_{exit} becomes large enough to cause substantial O₂ leakage and T_{max} reduction. When u_{exit} is at the upper part of its cycle, the asymmetry observed in the lower part of the cycle is not seen anymore, and the flame responds to the u_{exit} variations according to mechanism of O₂ leakage; the T_{max} values are in all cases lower compared to the ones resulting from adiabatic calculations. As the frequency increases, it can be seen that there is a tendency for "smoothing" of the T_{max} asymmetry in the low part of the u_{exit} cycle, and for frequencies higher than about 5 Hz the T_{max} variation with t' is controlled by the mechanism of O₂ leakage. This indicates that the characteristic time of oscillations becomes comparable to the characteristic time for the flame cooling as caused by the thermal radiation loss. Calculations were conducted for the determination of the characteristic cooling time, t_{cool} , of the flame, by dividing the local energy density throughout the flame by the rate of the radiative loss, q''' . Results are shown in Fig. 5b, and it can be seen that at the vicinity of the maximum flame temperature, t_{cool} assumes values at the vicinity of 0.25 to 0.75 sec. This explains the fact that the mechanism of flame cooling due to the radiative loss couples with the imposed oscillations at frequencies of the order of 2 to 4 Hz.

Summary

Weakly-burning flames are particularly sensitive to the complex interactions between aerodynamic straining, unsteadiness, chemical kinetics and radiative losses. The use of the counterflow technique for the independent probing of such effects can provide a whole new dimension in our understanding of these complex phenomena.

Acknowledgements

This research is supported by NASA under the technical supervision of Dr. Fletcher Miller of the Lewis Research Center.

References

1. Law, C.K. and Egolfopoulos, F.N. (1992). A Unified Chain-Thermal Theory of Fundamental Flammability Limits. *Twenty-Fourth Symposium (International) on Combustion*, Combustion Institute, p. 137.
2. Egolfopoulos, F. N. (1994) Geometric and Radiation Effects on Steady and Unsteady Strained Laminar Flames. To appear in the Proceedings of the *Twenty-Fifth Symposium (International) on Combustion*, Combustion Institute.
3. Williams, F.A. (1985). *Combustion Theory*, 2nd ed. Benjamin-Cummings, Menlo Park, California.
4. Ronney, P.D. (1988). On the Mechanisms of Flame Propagation Limits and Extinction Processes at Microgravity. *Twenty-Second Symposium (International) on Combustion*, Combustion Institute, p. 1615.
5. Ronney, P.D. (1988). Effect of Chemistry and Transport Properties on Near-Limit Flames at Microgravity. *Combust. Sci. Tech.* 59, 123.
6. Law, C.K. (1989). Dynamics of Stretched Flames. *Twenty-Second Symposium (International) on Combustion*, The Combustion Institute, 1381-1402.
7. Egolfopoulos, F.N., Cho, P., and Law, C.K. (1989). Laminar Flame Speeds of Methane-Air Mixtures Under Reduced and Elevated Pressures. *Combust. Flame* 76, 375-391.
8. Kreutz, T.G., Nishioka, N. and Law, C.K. (1994). The Role of Kinetic Versus Thermal Feedback in Nonpremixed Ignition of Hydrogen Versus Heated Air. To appear in the Proceedings of the *Twenty-Fifth Symposium (International) on Combustion*, Combustion Institute.
9. Law, C.K. and Egolfopoulos, F.N. (1990). A Kinetic Criterion of Flammability Limits: The C-H-O-Inert System. *Twenty-Third Symposium (International) on Combustion*, Combustion Institute, p. 413.
10. Egolfopoulos, F.N. (1994). Dynamics and Structure of Unsteady, Strained, Laminar Premixed Flames. To appear in the Proceedings of the *Twenty-Fifth Symposium (International) on Combustion*, Combustion Institute.
11. Kee, R.J., Rupley, F.M. and Miller J.A. (1989). Chemkin-II: A Fortran Chemical Kinetics Package for the Analysis of Gas-Phase Chemical Kinetics. *Sandia Report SAND89-8009*.
12. Kee, R.J., Warnatz, J., and Miller J.A. (1983). A FORTRAN Computer Code Package for the Evaluation of Gas-Phase Viscosities, Conductivities, and Diffusion Coefficients. *Sandia Report SAND83-8209*.

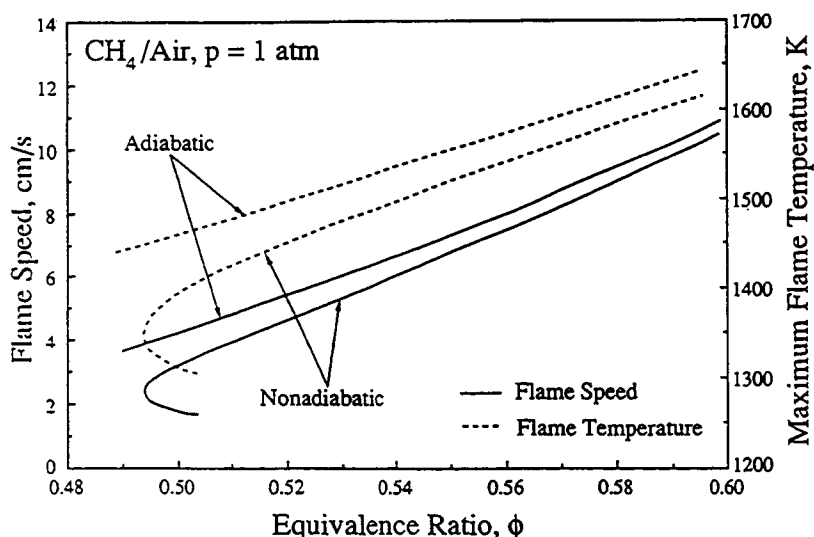


Figure 1. Effects of equivalence ratio and radiation on one-dimensional, steady, planar, lean premixed flames

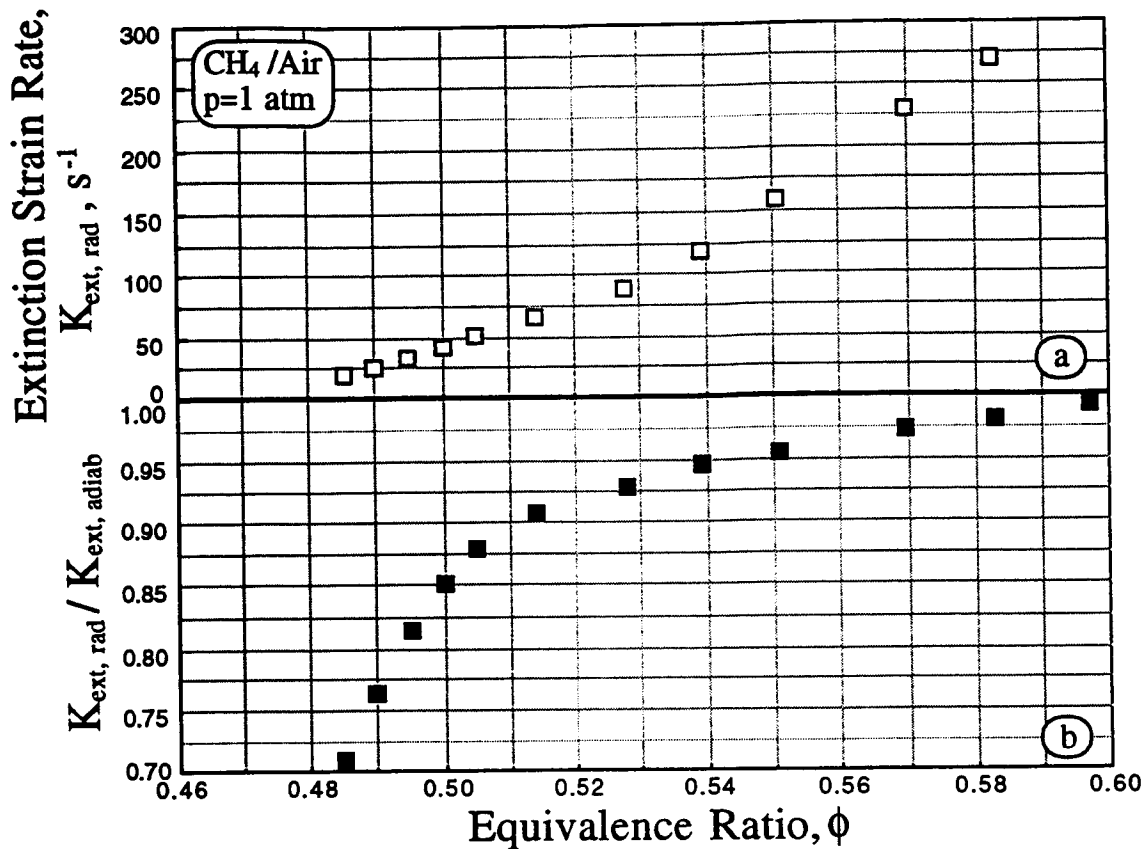


Figure 2. Effects of equivalence ratio and radiation on the extinction of steady, strained, lean premixed flames

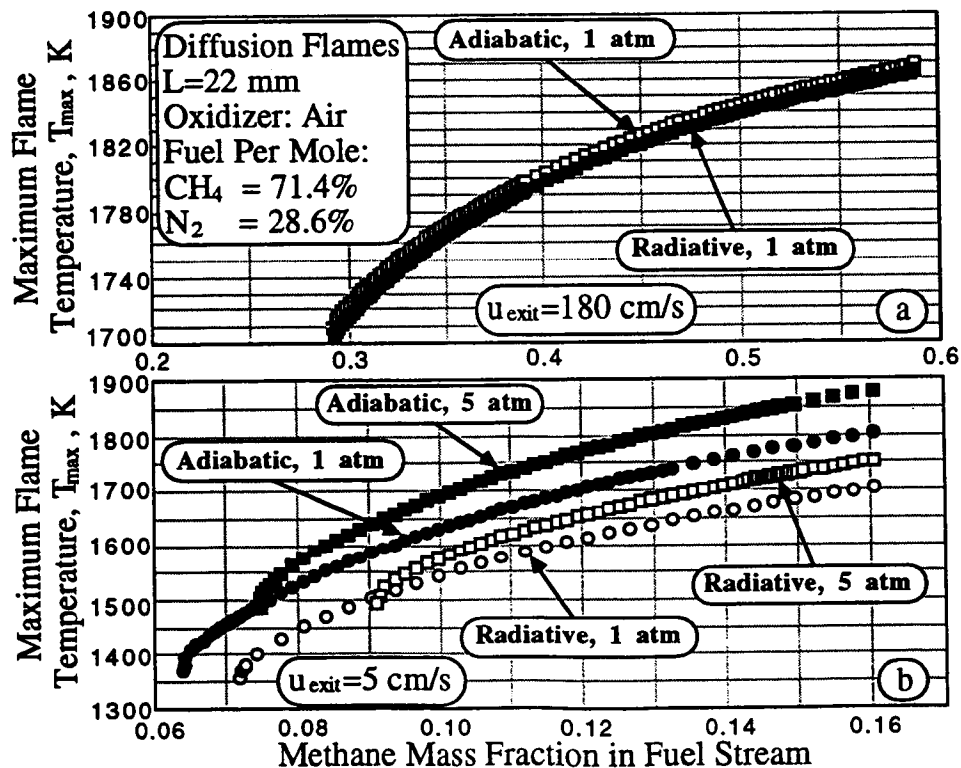


Figure 3. Effects of radiation and pressure on weakly and substantially strained diffusion flames

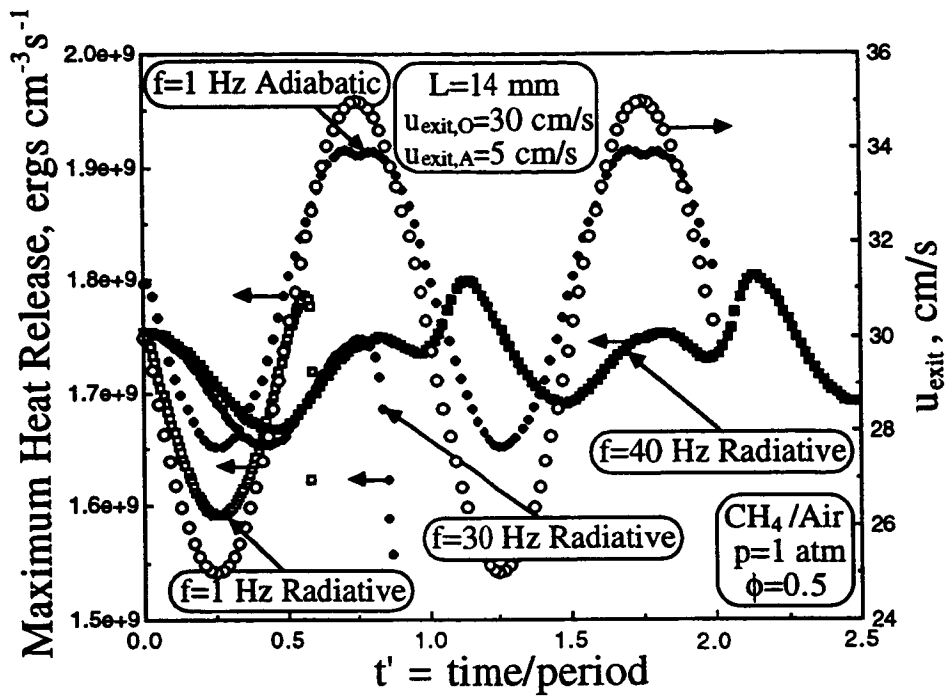


Figure 4. Effects of radiation and frequency on unsteady, strained, lean premixed flames

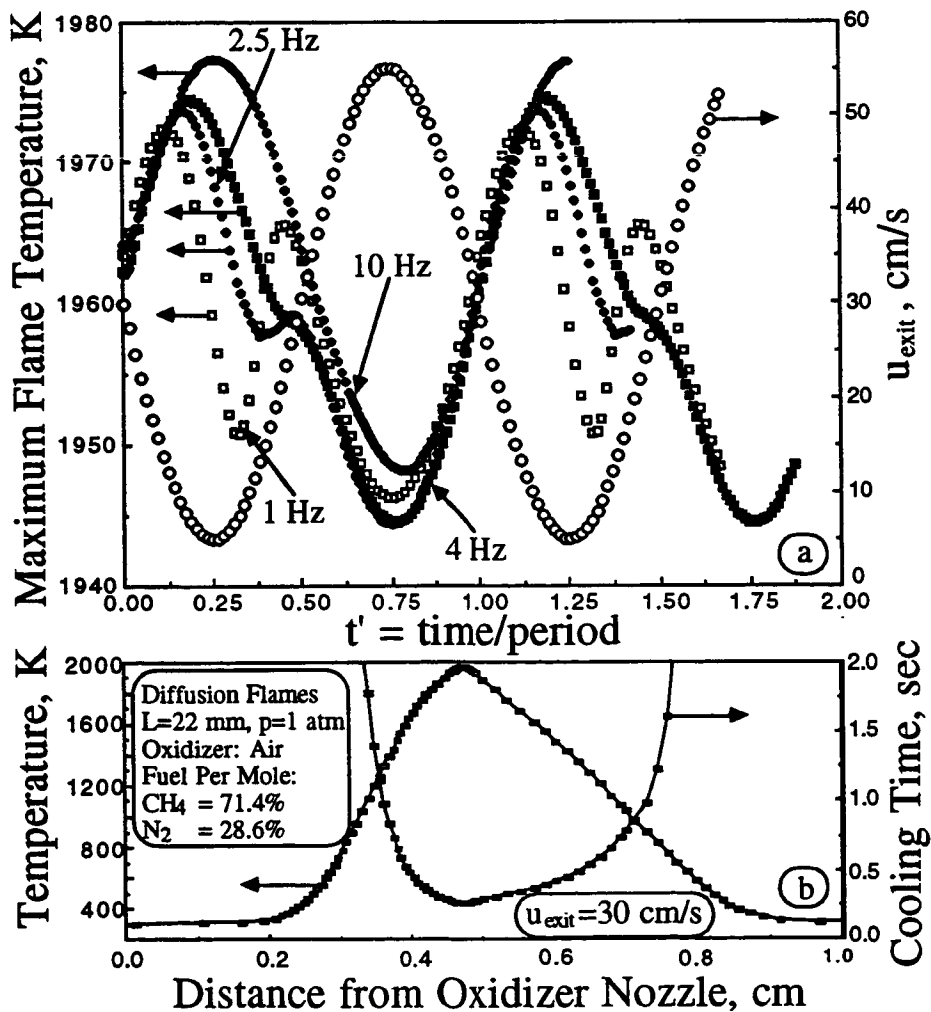


Figure 5. Effects of radiation and frequency on unsteady, strained, diffusion flames